Fauna and Systematics

Zoodiversity, 59(5): 383–398, 2025

DOI 10.15407/zoo2025.05.383
UDC 595.461(569.5)

DESCRIPTION OF A NEW SPECIES OF *ANDROCTONUS* (SCORPIONES, BUTHIDAE) FROM JORDAN

E. A. Yağmur [1, *], M. Al-Saraireh [2] & B. Abu Afifeh [3]

[1] Manisa Celal Bayar University, Alaşehir Vocational School, Alaşehir, Manisa, 45600 Turkey
[2] Oncology Department, Royal Medical Services, Amman, Jordan
[3] Ministry of Education, Al Rumman Secondary School, Amman, Jordan
* Corresponding author

E-mail: ersen.yagmur@gmail.com

E. A. Yağmur (https://orcid.org/0000-0002-0396-3975)
M. Al-Saraireh (https://orcid.org/0000-0002-0560-5469

urn:lsid:zoobank.org:pub:2A50B67E-B546-48E4-9F82-2CEA3A777D9D

Description of a New Species of *Androctonus* (Scorpiones, Buthidae) from Jordan. Yağmur, E. A., Al-Saraireh, M., Abu Afifeh, B. — A new scorpion species, *Androctonus ammoneus* sp. n., is described and illustrated from Zarqa Province, Jordan. Previous reports classified several *Androctonus* populations in Jordan as *A. crassicauda.* However, a comparative analysis with the neotype of *A. crassicauda* and other related species from Turkey and the Middle East reveals that *A. ammoneus* sp. n. is widely distributed in Jordan and represents a distinct species. The key distinguishing features include the chela structure and slenderness, metasomal carination, telson structure and general coloration. This study provides a comprehensive description and detailed illustrations of the new species, contributing to the taxonomic understanding of the genus *Androctonus* in the region.

Key words: Buthidae, new species, Jordan, taxonomy, Middle East.

Introduction

Scorpions of the genus *Androctonus* are among the most widely distributed and medically significant arachnids in North Africa, the Middle East, and western Asia (Fet & Lowe, 2000). The genus was first established by Ehrenberg in 1828, with *Scorpio australis* Linnaeus, 1758 designated as the type species. Currently, 41 valid species are recognized within *Androctonus* (Rein, 2025), yet the taxonomy of many regional populations remains unresolved.

The systematic position of *Androctonus* populations in the Middle East remains unclear, as many specimens have been historically assigned to *Androctonus crassicauda* (Olivier, 1807) for nearly two centuries. This species has been originally described from Kashan (Iran) and widely reported across Armenia, Azerbaijan, Bahrain, Egypt (Sinai), Iran, Iraq, Jordan, Kuwait, Oman, Saudi Arabia, Syria, Turkey, the United Arab Emirates, and Yemen (El-Hennawy, 1992, Fet & Lowe, 2000; Hendrixson, 2006; Amr et al., 2021; Alshammari et al., 2024). However, most of these records are based on external morphological similarities rather than precise taxonomic analyses, leading to potential misidentifications.

In Jordan, early studies by Vachon (1966) and Wahbeh (1976) documented *A. crassicauda*, followed by additional records from Kinzelbach (1985), El-Hennawy (1988), Levy & Amitai (1980), and Amr et al. (1988, 2016, 2021). These reports identified Jordanian *Androctonus* specimens as *A. crassicauda*, although the holotype was not available for comparative analyses or the application of modern taxonomic techniques.

Recent taxonomic revisions in the region have challenged this traditional classification. Yağmur (2021) designated a neotype for *A. crassicauda* and described a new species, *Androctonus turkiyensis*, from Turkey. Subsequent research led to the descriptions of additional species, including: *A. kunti* from Turkey (Yağmur, 2023), *A. tihamicus* from Saudi Arabia (Alqahtani et al., 2023) and *A. sumericus* from Iraq (Al-Khazali & Yağmur, 2023).

Further studies using molecular phylogenetics have revealed that *A. crassicauda* exhibits significant genetic heterogeneity across different populations. A study by Alqahtani et al. (2022) on Saudi Arabian *A. crassicauda* populations suggested the presence of cryptic species, which may explain the shortage of clear morphological distinctions among Middle Eastern populations. This genetic variability highlights the need for a taxonomic reassessment of *Androctonus* populations in Jordan and the broader region.

This study aims to clarify the taxonomic status of Jordanian *Androctonus* populations, particularly those previously identified as *A. crassicauda*. Through a detailed morphological examination of newly collected specimens, we describe a new species; *Androctonus ammoneus* **sp. n.**, from Jordan. Comparative analyses are conducted with the neotype of *A. crassicauda* and other related species from Turkey and the Middle East to determine distinguishing morphological characteristics.

This research contributes to the ongoing efforts to resolve taxonomic uncertainties in Middle Eastern *Androctonus* species, improving our understanding of their distribution, evolutionary relationships, and ecological significance.

Material and Methods

A total of 31 specimens of *A. ammoneus* **sp. n.** were collected during night using ultraviolet light from various habitats in Jordan. The collected scorpion specimens were preserved in 96% alcohol. The focus stacking method is modified from Canon-Cognisys system recommended by Brecko et al. (2014) and photographs were taken as proposed in Yağmur (2021). The trichobothrial nomenclature is after Vachon (1974) and morphological nomenclature after Francke (1977), Stahnke (1971) and Hjelle (1990). The male holotype and a male paratype and four female paratypes of *A. ammoneus* **sp. n.** were deposited in Alaşehir Zoological Museum, Manisa Celal Bayar University, Alaşehir, Manisa, Turkey (AZMM). Other paratypes are deposited in the private collection of Bassam Abu Afifeh (BAPC).

Results

Family **Buthidae**
Genus ***Androctonus***
***Androctonus ammoneus* sp. n.** (Figs 1–72, 75–81; Table 1)

urn:lsid:zoobank.org:act:486A7A34-DCF0-41C7-8197-641547507365

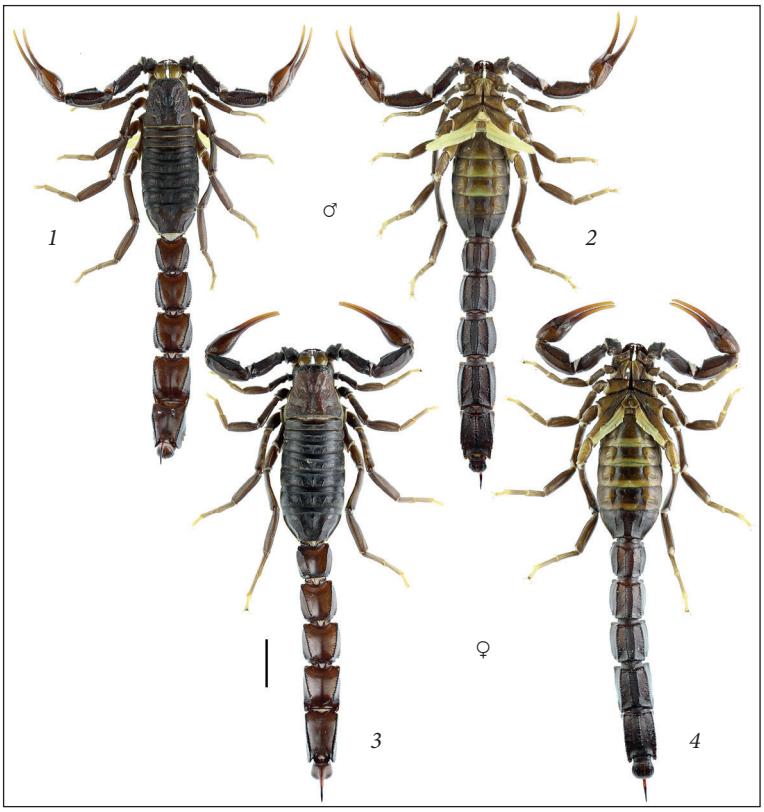

Figs 1–4. *Androctonus ammoneus* **sp. n.**, habitus. *1, 3* — dorsal views; *2, 4* — ventral views; *1–2* — holotype ♂; *3–4* — paratype ♀. Scale bar: 10 mm

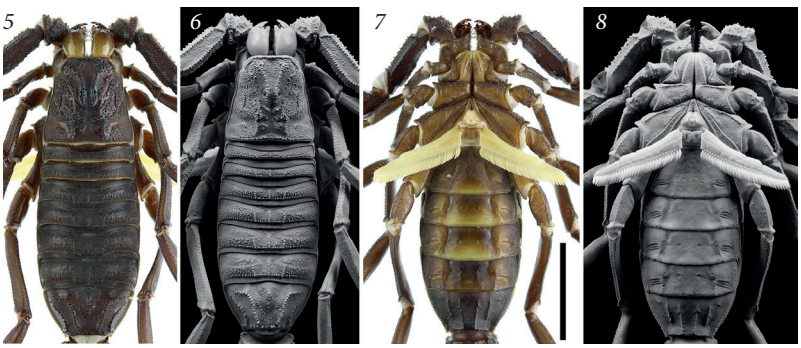

Figs 5–8. *Androctonus ammoneus* **sp. n.**, male holotype. *5–6* — carapace and mesosoma in dorsal view; *7–8* — mesosoma in ventral view and sternopectinal area; *5, 7* — under white light; *6, 8* — under UV light. Scale bar: 10 mm

Androctonus crassicauda: Vachon,1966: 210; Wahbeh, 1976: 90; Amr et al., 1988; 373; El-Hennawy, 1988: 17; Amr & El-Oran, 1994: 187; El-Hennawy, 1992: 97; Amr & Abu Baker, 2004: 238; Amr et al., 2016: 32; Amr et al., 2021: 88, 94.

Material examined. Holotype ♂: Jordan, Balqa Governorate, Ain Albasha, Um Al Dananeer, 32°05'34.6" N, 35°49'02.8" E, 768 m a. s. l., 12.08.2021, leg. B. Abu Afifeh (AZMM) — Paratypes: Jordan, Zarqa Governorate, Shaumari Nature Reserve, no exact locality, 11.05.1979, 1 ♀ (BAPC), leg. M. Failawi; Zarqa Governorate, Al-Rusaifa Cemetery, Hai Al-Rasheed, 32°01'25.8" N, 36°01'23.3" E, 614 m a. s. l., 1 ♀, 30.08.2018, leg. M. Al Saraireh, (BAPC); Amman Governorate, Sahab, inside

Table 1. **Measurements of morphological structures**

Dimensions, mm	Length (L), Width (W), Depth (D)	*Androctonus ammoneus* sp. n.	*Androctonus ammoneus* sp. n.
		♂ holotype	♀ paratype
Carapace	L / W	8.89 / 9.13	11.04 / 12.06
Mesosoma	L	18.17	26.07
Tergite VII	L / W	3.71 / 6.18	6.70 / 12.07
Metasoma + telson	L	47.27	57.27
Segment I	L / W / D	5.87 / 6.36 / 5.51	7.51 / 7.68 / 6.48
Segment II	L / W / D	6.87 / 6.81 / 5.85	8.27 / 7.77 / 7.24
Segment III	L / W / D	7.35 / 7.37 / 6.21	8.66 / 8.10 / 7.38
Segment IV	L / W / D	9.02 / 7.11 / 6.17	10.17 / 7.80 / 7.34
Segment V	L / W / D	9.99 / 6.13 / 4.58	11.16 / 6.87 / 5.67
Telson	L / W / D	8.17 / 2.12 / 2.58	11.50 / 3.24 / 3.55
Pedipalp	L	32.5	38.33
Femur	L / W	7.92 / 2.42	9.03 / 3.11
Patella	L / W	9.05 / 3.37	10.62 / 4.36
Chela	L	15.53	18.68
Manus	L / W / D	6.09 / 3.61 / 4.03	6.98 / 4.23 / 4.72
Fixed Finger	L	8.41	10.31
Movable finger	L	10.29	12.56
Total	L	74.33	94.38

abandoned house, 31°49'14.0" N, 36°01' 34.7" E, 773 m a. s. l., 2 ♂, 13.09.2019, leg. M. Al-Saraireh (BAPC); Amman Governorate, Ghor Sweimeh near Dead Sea, 31°46'13.3" N, 35°35'21.2" E, 365 m a. s. l., 3 ♀, 5.07.2020, leg. M. Al-Saraireh (BAPC); Balqa Governorate, Ain Albasha, Um Al Dananeer, 32°05'34.6" N, 35°49'02.8" E, 768 m a. s. l., 3 ♂, 6 ♀, 25.04.2021, leg. B. Abu Afifeh, (BAPC), same place 1 ♀, 12.08.2021 (AZMM); Zarqa Governorate, 14 km SE of Al Azraq, Wadi Rajel (Wadi Qarma), 31°46'05.7" N, 36°57'26.5" E, 522 m a. s. l., 6 ♂, 2 ♀, 02.05.2022, leg. B. Abu Afifeh (BAPC); Karak Governorate, Wadi Araba, Wadi Al-Ghwaibeh, 30°48'07.9" N, 35°22' 59.0" E, -153 m a.s.l., 1 ♀, 07.04.2022, leg. B. Abu Afifeh, R. Abu Afifeh & M. Al Saraireh (BAPC), 1 ♀ (AZMM); Aqaba Governorate, 12 km SE of Al Ghal / Wadi Rum, 29°27'02.0" N, 35°41'19.5" E, 873 m a. s. l., 1 ♀, 15.07.2022, leg. B. Abu Afifeh & R. Abu Afifeh (BAPC), 1 ♀ (AZMM); Aqaba Governorate, Ports highway / 8 km SE Aqaba, 29°29'23.1" N, 35°04'55.7" E, 710 m a. s. l., 1 ♀, 21.08.2023, leg. M. Al-Saraireh, (BAPC); Zarqa Governorate, 19 km E of Al Azraq, 31°47'57.6" N, 37°00'28.4" E, 530 m a. s. l., 1 ♀, 12.09.2023, leg. B. Abu Afifeh (BAPC); Mafraq Governorate, Marab Aroos, 32°07'33.9" N, 37°20'37.8" E, 660 m a. s. l., 1 ♀, 07.10.2024, leg. B. Abu Afifeh (BAPC); Balqa Governorate, Al Rumman, 32°09'56.0" N, 35°49'50.4" E, 557 m a. s. l., 1 ♀, 08.11.2024, leg. B. Abu Afifeh, (BAPC); Zarqa Governorate, Rajm Ashouf, 32°04'38.5" N, 35°57'28.7" E, 1 ♀, 03.06.2024, leg. M. Al Saraireh (BAPC).

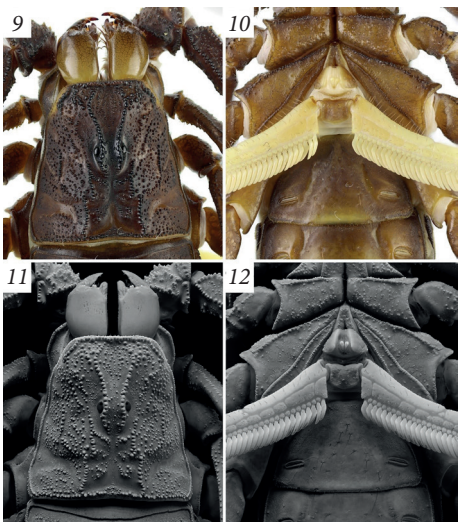

Figs 9–12. *Androctonus ammoneus* **sp. n.**, male holotype. *9, 11* — carapace; *10, 12* — sternopectinal area; *9–10* — under white light; *11–12* —under UV light

Etymology. The specific epithet *ammoneus* is derived from the Ammonites, an ancient Semitic people who established the Kingdom of Ammon in what is now Jordan.

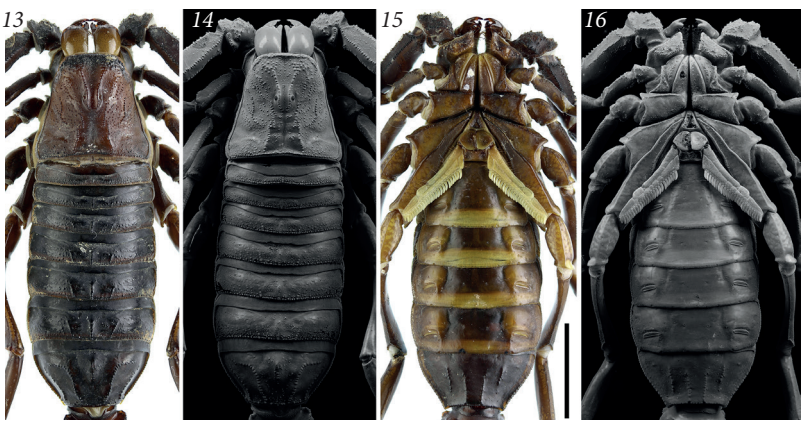

Figs 13–16. *Androctonus ammoneus* **sp. n.**, female paratype. *13–14* — carapace and mesosoma in dorsal view; *15–16* — Mesosoma in ventral view and sternopectinal area; *13, 15* — under white light; *14, 16* — under UV light. Scale bar: 10 mm

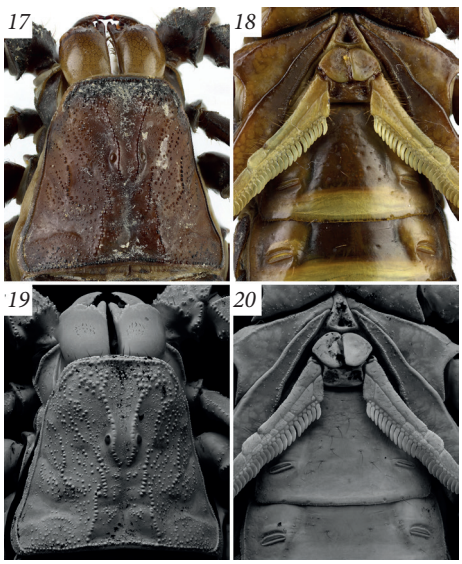

Figs 17–20. *Androctonus ammoneus* **sp. n.**, female paratype. *17, 19* — carapace; *18, 20* — sternopectinal area; *17–18* — under white light; *19–20* — under UV light

Figs 21–28. *Androctonus ammoneus* **sp. n.**, male holotype, pedipalp segments, under white light. *21* — chela ventral view; *22* — chela dorsal view; *23* — chela internal view; *24* — chela external view; *25* — pedipalp dorsal view; *26* — pedipalp ventral view; *27* — movable finger dentition; *28* — fixed finger dentition. Trichobothrial pattern is indicated by green circles

This kingdom thrived between the 10th century BC and 332 BC. The name reflects the geographical origin of the species and pays tribute to the rich history of Jordan.

Diagnosis. Medium-large sized scorpions. Size with males reaching up to 78 mm, and females up to 94 mm in total length. General coloration dark brown. Carapace carinae strong and coarsely granular. Intercarinal area covered with moderately dense coarse and rounded granules in males, granules less dense and slightly smaller in females. Chela smooth, lustrous and moderately slender, surface somewhat rough without carinae. Internal surface of manus densely granular in male, nearly smooth with a few minute granules in females. Fixed and movable fingers with 15 and 14 principal rows of denticles. Trichobothrium *et* is located between *dt* and *est*. Pectines with 29–34 teeth in males, and 24–27 in females. Tergites I–VI with three moderate and granular carinae, submedian carinae reduced in tergites I and II in male; carinae weak and granules flattened in females. Tergites I–VI coarsely granular in male; granules flattened and less dense in females. Surface between the submedian carinae shagreened with several medium granules. Tergite VII pentacarinate. Metasomal segments robust; segment I wider than long, segment II–V longer than wide. Metasomal segments I to III with 10, segment IV with 8, and segment V with 5 carinae. Dorsolateral carinae strong with gradually increased posteriorly granules on segments I–IV; serratocrenulate to serrate on segments I–II in male, crenulate in females; serrate on segments III–IV; strong, posteriorly crenulate, anteriorly smooth on segment V. Ventrolateral carinae strong on segments I–IV, with coarse, rounded granules; strong on segment V with gradually and slightly increased granules posteriorly with two slightly larger subconical denticles in male, two or three subspinoid or conical in females. Lateral surface rough and finely

granular on segments I–V, granulation denser on segment III–V with scattered medium granules in male, all segments almost smooth in females. Ventral surface rough and finely granular with scattered medium granules on segments I–V, but segments I–III with reticular granulations and smooth patches in male, almost smooth, on segment III–V weakly granular in females. Telson slender and elongated; aculeus long and thick, slightly shorter than the vesicle, and abruptly curved.

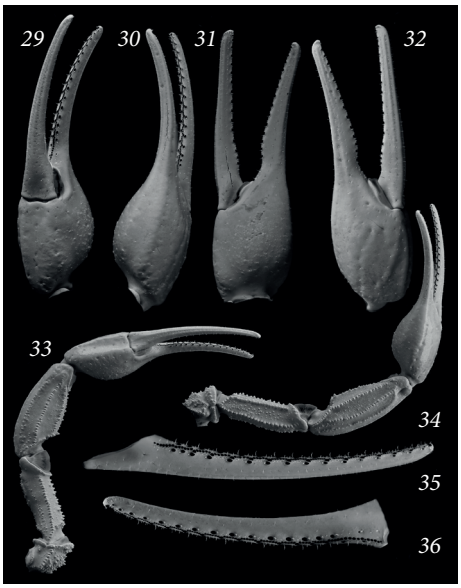

Figs 29–36. *Androctonus ammoneus* **sp. n.**, male holotype, pedipalp segments, under UV light. *29* — chela ventral view; *30* — chela dorsal view; *31* — chela internal view; *32* — chela external view; *33* — pedipalp ventral view; *34* — pedipalp dorsal view; *35* — movable finger dentition; *36* — fixed finger dentition

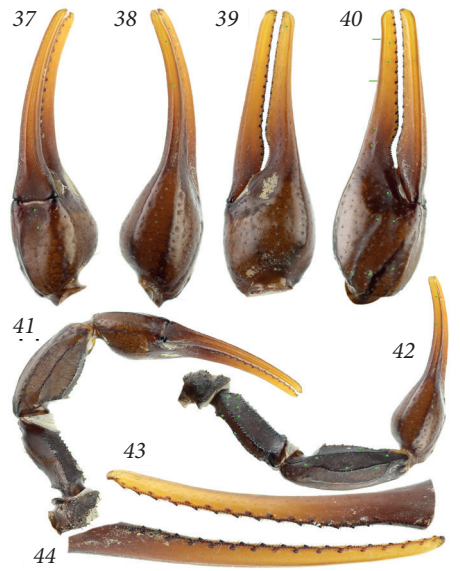

Figs 37–44. *Androctonus ammoneus* **sp. n.**, female paratype, pedipalp segments, under white light; *37* — chela ventral view; *38* — chela dorsal view; *39* — chela internal view; *40* — chela external view; *41* — pedipalp ventral view; *42* — pedipalp dorsal view; *43* — fixed finger dentition; *44* — movable finger dentition. Trichobothrial pattern is indicated by green circles

Affinities

The newly described species, *A. ammoneus* **sp. n.**, can be distinguished from other Middle Eastern *Androctonus* species based on key morphological features, including chela structure and selenderness, metasomal carination, telson structure and general coloration. The following diagnostic comparisons highlight its distinct characteristics:

1. Pedipalp chela slenderness:

A. ammoneus **sp. n.** exhibits relatively slender chela; chela length to width ratio 4.30–5.48 in males (n = 6) (Figs *21–24*, *29–32*), and 4.41–4.93 in females (n = 5) (Figs *37–40*, *45–48*).

A. crassicauda has moderately slender chela; chela length to width ratio 3.80–4.06 in males (n = 2), and 4.06 in the female.

A. sumericus has a relatively robust chela; chela length to width ratio 3.35–3.54 in males (n = 2), and 3.29–3.88 in the females (n = 3).

2. Metasomal Carination:

The dorsolateral carinae of metasomal segment V in *A. ammoneus* **sp. n.** are crenulated to smooth (Fig. *75*), whereas in *A. crassicauda*, they are strongly serrated anteriorly (Fig. *73*).

The dorsolateral carinae of metasomal segments III–IV are coarse, well-defined, and highly pronounced in *A. crassicauda*

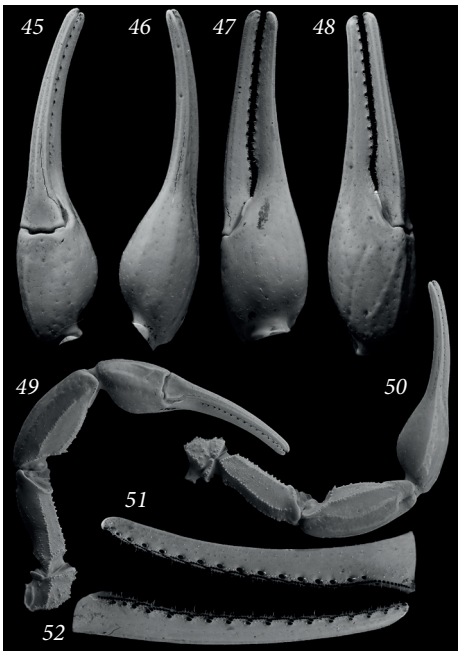

Figs 45–52. *Androctonus ammoneus* **sp. n.**, female paratype, pedipalp segments, under UV light. *45* — chela ventral view; *46* —Chela dorsal view; *47* — chela internal view; *48* — chela external view; *49* — pedipalp ventral view; *50* — pedipalp dorsal view; *51* — fixed finger dentition; *52* — movable finger dentition

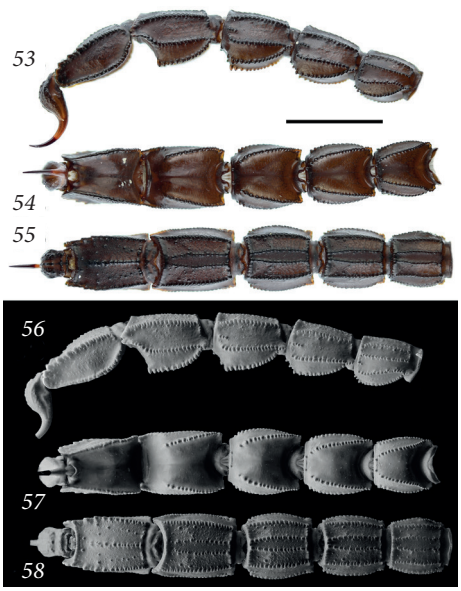

Figs 53–58. *Androctonus ammoneus* **sp. n.**, metasoma and telson of male holotype. *53, 56* — lateral views; *54, 57* — dorsal views; *55, 58* — ventral views; *53–55* — under white light; *56–58* — under UV light. Scale bar: 10 mm

(Fig. *73*), featuring strong, irregular granules that form a serrated or saw-like appearance. In *A. turkiyensis* (Fig. *74*), they are moderately developed, with smaller, more evenly spaced granules. In contrast, *A. ammoneus* **sp. n.** (Fig. *73*) exhibits the least pronounced carinae, appearing more rounded and less serrated.

The ventrolateral carinae of segment V in *A. ammoneus* **sp. n.** bear 2–3 subconical or subspinoid denticles (Figs *65–70*, *75*), whereas *A. crassicauda* lacks enlarged denticles (*73*).

The enlarged denticles on ventrolateral carinae of segment V in *A. kunti* and *A. turkiyensis* (Fig. *74*) are significantly larger than those in *A. ammoneus* **sp. n.**, whereas *A. sumericus* exhibits the smallest denticles among them.

3. Telson Structure:

The telson of *A. crassicauda* (Fig. *73*) is robust, featuring a thick structure with a strongly curved aculeus that appears darker at the tip. In *A. turkiyensis* (Fig. *74*), the telson remains curved but is somewhat less robust than in *A. crassicauda*, with a vesicle that appears slightly more elongated. In contrast, *A. ammoneus* **sp. n.** (Fig. *75*) has the most elongated and curved telson among the three species, giving it a more slender and flexible appearance.

4. Chela Fingers Gap:

In *A. ammoneus* **sp. n.** the chela exhibits an indistinct gap between fingers (Figs *24, 32, 40, 48, 76–79*).

In *A. sumericus*, the chela has a distinct gap between fingers (Al-Khazali and Yağmur, 2023, Fig. 4, d).

In *A. bicolor* chela without basal lobe/notch combination between fingers (Teruel and Kovařík, 2014, Figs 6, 8).

5. Coloration:

A. ammoneus **sp. n.** has a dark brown body coloration.

A. australis, A. amoreuxi, A. sumericus, and *A. tihamicus* are light brown to yellow.

A. crassicauda and *A. kunti* are black.

Description. Description is based on the male holotype and female paratypes. The total length in adults reaching 78 mm in males, and 94 mm in females. Measurements are given in Table I.

Coloration. Base color brown to dark brown. Prosoma: Carapace dark brown in male, dark brown to dark reddish brown in females; carinae and granules black blackish brown. Between and surround of median eyes marked by black pigmentation. Furrows lighter. Anteriolateral corners of carapace, in front of the lateral eyes, dark yellow (Figs *1–4, 9, 17*). Mesosoma: Dark brown to dark reddish brown. Posterior margins of tergites I–VI with dark yellow bands. Sternites III–V yellowish brown, dark and brilliant yellow medially and posteriorly. Sternite VI dark brown to yellowish brown. Sternite VII dark brown to blackish brown. Coxae yellowish brown, carina dark brown. Pectines pale light yellow (Figs *1–4, 5, 7, 13, 15*). Chelicerae: Manus shiny yellow to yellowish brown with dark brown variegated spots; fingers dark brown to reddish brown, teeth yellowish red with reddish black apex (Figs *9, 17*). Pedipalps: Femur dark brown dorsally, with blackish brown carinae and granules; patella dark reddish brown or brown with slight reticulations; chela manus lustrous reddish brown with dark brown spots and reticulations; fingers dark brown posteriorly, dark yellow anteriorly, the denticles black (Figs *21–28, 37–44*). Legs: Tarsi and basitarsus brownish yellow, pretarsus dark brownish yellow with brown reticular spots, rest segments brown (Figs *1–4, 71, 72*). Metasoma: Segments I to V brown with indistinct dark brown reticulations; carinae and granules marked dark brown or black pigmentation. Vesicle reddish black with reddish brown dorsal and lateral furrows; aculeus reddish brown at base and black at tip (Figs *53–55, 59–61, 65, 66*).

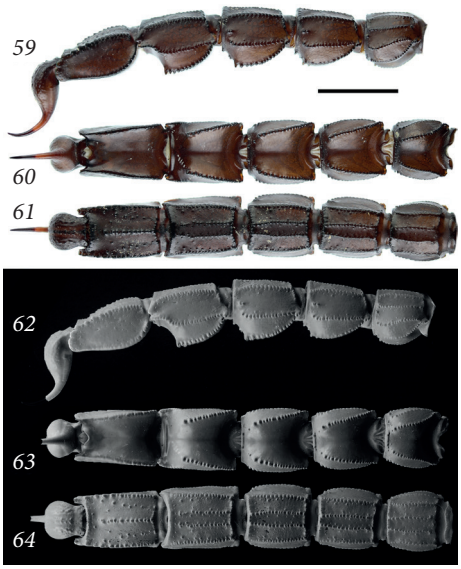

Figs 59–64. *Androctonus ammoneus* **sp. n.,** metasoma and telson of female paratype. *59, 62* — lateral views; *60, 63* — dorsal views; *61, 64* — ventral views; *59–61* — under white light; *62–64* — under UV light. Scale bar: 10 mm.

Morphology. Prosoma. Carapace trapezoidal, slightly wider than long. Carapace carinae strong and coarsely granular. Intercarinal area covered with moderately dense coarse and rounded granules in males, granules less dense and slightly smaller in females. Carapace anteromedian intercarinal surface with medium sized granules, and the area around and between median eyes with minute granules. Anterior area with denser larger and slightly flattened granules.

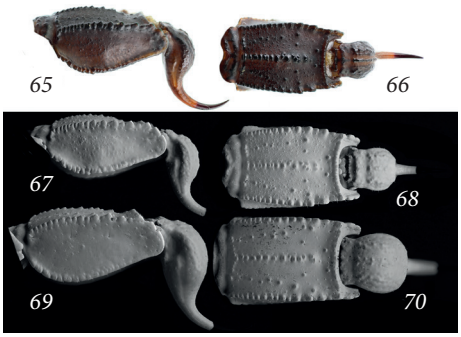

Figs 65–70. *Androctonus ammoneus* **sp. n.**, segment V of metasoma and telson. *65–68* — male holotype; *69–70* — female paratype; *65–66* — under white light; *67–70* — under UV light; *65, 67, 69* — lateral views; *66, 68, 70* — ventral views

Fig. 71. *Androctonus ammoneus* **sp. n.**, male holotype, tibia, basitarsus and tarsus of right legs I–IV

Fig. 72. *Androctonus ammoneus* **sp. n.**, female paratype, tibia, basitarsus and tarsus of right legs I–IV

Figs 73–75. Comparison metasoma III–V and telson from lateral aspect between *A. crassicauda* (*73,* male neotype from Iran, Kashan), *A. turkiyensis* (*74,* male holotype), and *A. ammoneus* **sp. n.** (*75,* male paratype)

Anterior margin nearly straight, with some stout macrosetae and coarse fixed granules. All furrows moderate and smooth. Median ocular tubercle slightly anterior to the center of carapace; median eyes separated by two ocular diameters. Five pairs of lateral eyes, the first three of moderate size and aligned and above area with moderate granules, the last two vestigial (Figs *9, 11, 17, 19*).

Sternum standard for the genus: type 1, triangular and narrow, longer than wide, apex shrinks (Figs *10, 12, 18, 20*).

Genital operculum divided longitudinally, forming two semi-oval plates; Pectines long, well passing leg IV coxa/trochanter joint in male barley reach but not pass in females. Narrow and densely setose; tooth count 31–32 in male holotype, 24–27 in females; basal plate heavily sclerotized and wider than long, anterior margin with strong median indentation, posterior margin widely convex.

Chelicerae. Cheliceral dentition typical for the genus as defined by Vachon (1963); teeth short with sharp apex; surface smooth and lustrous with granules arranged in longitudinal ridges setae cluster exist under the moving finger (Figs *9, 11, 17, 19*).

Pedipalps. The trichobothrial pattern is of Type A, orthobothriotaxic. The dorsal trichobothria of the femur are arranged in a beta-configuration, with *d2* situated on the dorsal surface. Femur is pentacarinate, moderately slender and straight. The dorsointernal, dorsoexternal, and ventrointernal carinae are strong, with coarse and rounded granules. The ventroexternal carinae are weak, with moderate, spaced subspinoid granules, while the internal median carinae are weak, with spaced distinct conical granules. The dorsal intercarinal surface is finely granular, with moderate rounded granules medially, whereas the ventral intercarinal surface is smooth, with scattered minute granules and medium conical granules in the anterior two-thirds of the segment. Pa-

Figs 76–79. Trichobothria arrangement variations on the chela fixed fingers of *Androctonus ammoneus* **sp. n.** *76* — male holotype; *77* — female paratype from Balqa; *78* — Male paratype from Zarqa; *79* — female paratype from Zarqa

tella has eight carinae, is moderately slender and straight, and features strong dorsointernal, dorsal, and ventrointernal carinae. The dorsomedian, ventromedian and exteriomedian carinae are moderate, while the dorsoexternal, and ventroexternal carinae are weak. The dorsal, dorsomedian, and ventromedian carinae have coarse and rounded granules, whereas the dorsoexternal and ventroexternal carinae are weakly granular to smooth. The dorsointernal and ventrointernal carinae are crenulate, with three or four conical granules terminating in one large spinoid granule distally. Exteriomedian carinae smooth. The dorsal intercarinal surface is finely granular, with moderate granules medially, while the ventral intercarinal surface has granules of varied sizes. Chela is smooth, lustrous, and moderately slender (chela length/manus width ratio = 4.30 in male holotype, 4.42 in female paratype), with a somewhat rough surface and no carinae. The manus is slightly wider than the patella in male holotype (chela width/patella width = 1.07), and slightly narrower in female paratype (chela width/patella width = 0.97). The internal surface of the manus is densely granular in males but nearly smooth, with a few minute granules in females. Fingers are moderately elongated (movable finger length/manus length ratio = 1.69 in male holotype, 1.80 in female paratype) and evenly curved. The movable finger of the pedipalp bears three distal denticles and 15 principal rows of denticles, along with external and internal accessory denticles. The fixed finger has two distal denticles, and 14 principal rows of denticles, external and internal accessory granules, and three distal granules. Trichobothrium *et* is located between *dt* and *est*, closely positioned to *dt*. Trichobothrium *est* is located between *et* and *db*, though its position varies. In some specimens, *est* is located closely to *db*, while in others, it is positioned midway between *et* and *db* (Figs *21–52*).

Legs. Legs long, slender, and covered with macrosetae. The basitarsus of legs I to III has bristlecombs, whereas the basitarsus of leg IV lacks bristlecombs. Proventral and retroventral basitarsal (pedal) spurs are present on legs I and IV, while tibial

spurs are present on legs III and IV. Tarsus of legs I–IV is ventrally covered with spine-like setae arranged in two rows (Figs *71, 72*).

Mesosoma. Tergites I–VI with three moderate and granular carinae (median and submedians), submedian carinae reduced in tergites I and II in male; carinae weak and granules flattened in females. Tergites I–VI coarsely granular in male; granules flattened and less dense in females. Pretergits with medium and fine granules in tergites I–VI in male; somewhat smooth in females. Surface between submedian carinae shagreened with several medium granules. Posterior margins with a row of distinct moderate granules. Tergite VII pentacarinate (median, submedians and laterals); median and submedians bear coarse and rounded granules; laterally serrated with subspinoid granules. Surface between submedian carinae shagreened with several medium granules, rest surface finely granular in tergite VII in male; between submedian carinae with scattered minute granules, rest surfaces almost smooth. Sternites III–VI smooth, sparsely setose, and spiracles slit-like and elongated. Sternite III shagreened on the sides with shagreened patches. Sternites IV–VI with a couple of obsolete and weak carinae. Sternite VII with two couple of moderate and weakly granular carinae. Sternite VII smooth and sparsely setose with finely granular patches (Figs *5–8, 13–16*).

Metasoma. Segments robust; segment I wider than long, segment II–V longer than wide and all segments wider than deep. Metasomal segments I to III with 10, segment IV with 8, and segment V with 5 carinae. Lateral inframedian carinae complete, moderate, and granular on segment I, incomplete, present on posterior quarter, weakly granular (consists of 3–4 granules) on segment II–III. Dorsolateral carinae strong with gradually increased granules posteriorly on segments I–IV; serrato-crenulate to serrate on segments I–II in male, crenulate in females; serrate on segments III–IV; strong, posteriorly crenulate, anteriorly, smooth on segment V. Lateral supramedian carinae strong and granular on I–IV with moderate, rounded granules. Ventrolateral carinae strong on segments I–IV, with coarse, rounded granules; strong on segment V with gradually and slightly increased granules posteriorly with two slightly larger subconical denticles in male, two or three subspinoid or conical in females. Ventral submedian carinae moderate and granular on segments I–IV. Ventromedian carina moderate on segments V, with moderate rounded granules, bifurcated at the posterior portion. Anal arch has two rounded lateral lobes, with the inferior lobe being twice as large as the superior one. Metasoma is very sparsely setose. Intercarinal area on the dorsal surface finely granular mesially on segment I, while segments II–V are smooth and lack granulation. The lateral surface is rough and finely granular across segments I–V, with denser granulation on segments III–V in male, whereas all segments appear almost smooth in females. Ventral surface is rough and finely granular, with scattered medium granules on segments I–V. However, in males, segments I–III feature reticular granulation and smooth patches, while in females, segments III–V are weakly granular and mostly smooth. The dorsal surface is generally smooth, except for segment I, which has fine medial granules. Dorsal furrow is moderately deep and wide across all segments. Telson slender and elongated; vesicle somewhat thin and elongated, tegument rough but surface smooth, with distinct and obsolete ventromedian carinae; aculeus long and thick, shorter than vesicle (vesicle/aculeus ratio = 1.24) and abruptly curved (Figs *53–70*).

Discussion

Scorpions of the genus *Androctonus*, commonly known as fat-tailed scorpions, are among the most medically significant scorpions due to their highly potent venom. Found primarily in North Africa, the Middle East, and parts of Asia, these scorpions pose a serious health risk, particularly in arid and semi-arid regions (Chippaux & Goyffon, 2008). Their venom is rich in neurotoxins, including powerful α- and β-toxins that target sodium and potassium ion channels, leading to severe envenomation (Bosmans et al., 2006). *Androctonus* species, including *A. crassicauda* and *A. australis*, are responsible for numerous scorpion sting fatalities each year, prompting the development of specific antivenoms to mitigate their effects (Ismail, 1995; Amr et al., 2021).

Updates on the classification and taxonomy of *Androctonus* species are crucial for understanding intraspecific variations within this genus. A deeper knowledge of these differences can contribute to more targeted antivenom production, improving treatment effectiveness and reducing fatalities.

The findings of this study highlight the need for a revision and re-examination of other *Androctonus* species previously reported from Jordan, such as *A. bicolor*, *A. amoreuxi*, and *A. australis* (El-Hennawy, 1988; Amr & El-Oran, 1994; Amr et al., 2016; Seiter & Turiel, 2013). Reassessing these records may provide further insights into their taxonomy, distribution, and medical significance.

Comment on Trichobothrial Variation. Trichobothria are highly conserved sensory structures in scorpions and serve as important taxonomic markers (Soleglad & Fet, 2001). The genus *Androctonus* follows a Type A trichobothrial pattern, typical for the family Buthidae, which is generally stable within species and widely used for classification. However, our findings reveal notable intraspecific and intra-individual variation in the positioning of trichobothria *et* and *est* in *A. ammoneus* **sp. n.**

Observations from multiple specimens (Figs *76–79*) indicate two main types of positional variation:

1. Trichobothrium *et*: Located either proximally to *dt* or midway between *dt* and *est*.
2. Trichobothrium *est*: Found either proximally to *db* or between *et* and *db*.

Interestingly, asymmetry was also noted in some individuals, where the left and right chelae exhibited different trichobothrial positions (Figs *80, 81*). This raises questions about the consistency of trichobothria as a diagnostic trait within *Androctonus*.

Trichobothrial position variability has been occasionally documented in other Old World scorpion genera of Buthidae. Navidpour et al. (2008) reported intraspecific variation in *Orthochirus*, specifically in trichobothria d_2 and e_1. Sousa et al. (2017) observed both interspecific and intraspecific differences in *Buthus*, questioning the reliability of trichobothrial position for species identification in that genus.

Given these findings, the taxonomic significance of trichobothrial position in *A. ammoneus* **sp. n.** should be interpreted cautiously. While *Androctonus* generally exhibits stable trichobothrial patterns, the observed variability in *et* and *est* position suggests that these structures should not be the sole diagnostic criterion for

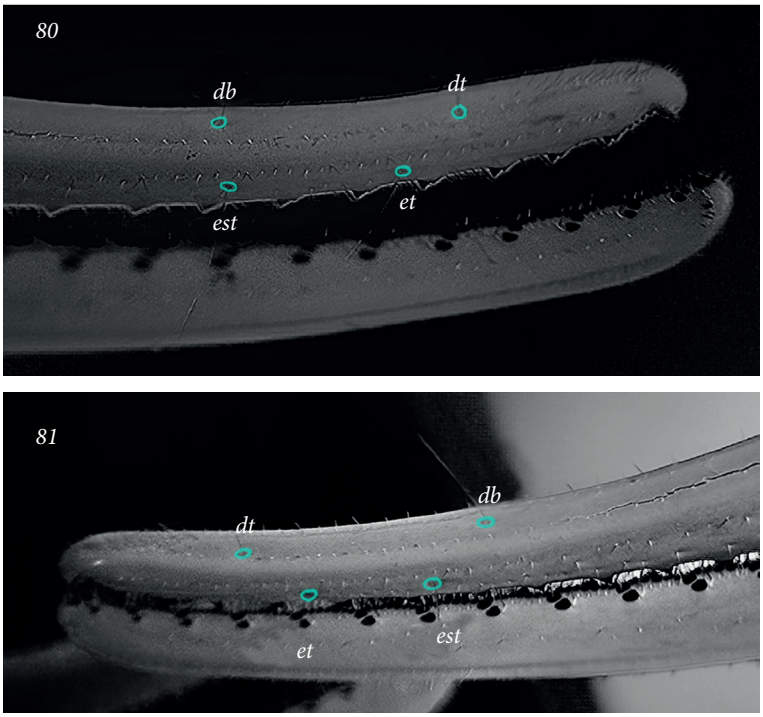

Figs 80–81. Variation of trichobothrial positions among both pedipaps of the same *Androctonus ammoneus* **sp**. **n**. Female paratype. *80* — right chela; *81* — left chela

species delineation. In our study, a combination of carinal morphology, chela structure, and metasomal features were used to differentiate *A. ammoneus* **sp. n.** from closely related species.

Ecology. This species is widely distributed across various habitats in Jordan, with particularly high abundance in the eastern desert, as well as in Wadi Araba, Aqaba, and Wadi Rum. It has also been recorded in the Mediterranean region at higher altitudes and in areas with significant annual rainfall, though in lower numbers. The presence of this species in diverse environments suggests a high degree of ecological adaptability, allowing it to persist in both arid and semi-arid landscapes as well as more temperate regions.

According to our observations, this species exhibits a tendency to inhabit human-modified environments, including old homes, abandoned structures, and areas around Bedouin campsites and tented settlements. This behavior significantly increases the likelihood of human encounters and subsequently poses a potential public health concern.

Furthermore, its presence across different ecological zones highlights the need for further studies on its behavioral patterns and population dynamics. Understanding its distribution and habitat preferences can contribute to the development of effective mitigation strategies, including public awareness campaigns and preventive measures to reduce the risk of scorpion stings in vulnerable communities.

REFERENCES

Al-Khazali, A. M. & Yağmur, E. A. 2023. *Androctonus sumericus* sp. nov., a new scorpion from Dhi Qar Province, Iraq (Scorpiones: Buthidae). *Zoology in the Middle East*, **69** (4), 410–419. https://doi.org/10.1080/09397140.2023.2284016.

Alqahtani, A. R., Badry, A., Amer, S. A., Galil, F. M. A., Ahmed, M. A. & Amr, Z. S. 2022. Intraspecific molecular variation among *Androctonus crassicauda* (Olivier, 1807) populations collected from different regions in Saudi Arabia. *Journal of King Saud University — Science*, **34** (4), 101998. https://doi.org/10.1016/j.jksus.2022.101998.

Alqahtani, A. R., Yağmur, E. A. & Badry, A. 2023. *Androctonus tihamicus* sp. nov. from the Mecca Province, Saudi Arabia (Scorpiones, Buthidae). *ZooKeys*, **1152,** 9–34. https://doi.org/10.3897/zookeys.1152.101100.

Alshammari, M. M., Abu Afifeh, B., Al-Quraan, N., Abuharfil, N. M. & Amr, Z. S. 2024. Scorpions of the State of Kuwait. *Ecologica Montenegrina*, **75,** 52–66. https://doi.org/10.37828/em.2024.75.4.

Amr, Z. S., Abed, O. A., Al Share, T., Hamidan, N. & Prendini, L. 2016. New records of Jordanian scorpions. *Jordan Journal of Natural History*, **2,** 30–38.

Amr, Z. S. & Abu Baker, M. A. 2004. The scorpions of Jordan. *Denisia*, **14,** 237–244.

Amr, Z. S., Abu Baker, M. A., Al-Saraireh, M. & Warrell, D. A. 2021. Scorpions and scorpion sting envenoming (scorpionism) in the Arab Countries of the Middle East. *Toxicon,* **191,** 83–103.

Amr, Z. S. & Al-Oran. R, 1994. Systematics and distribution of scorpions (Arachnida, Scorpionida) in Jordan. *Bollettino di Zoologia*, **61,** 185–190.

Amr, Z., Hyland, K. Kinzelbach, R. Amr, S. & Defosse, D. 1988. Scorpions et piqûres de scorpions en Jordanie. *Bulletin de la Société de Pathologie Exotique*, **81,** 369–379.

Brecko, J., Mathys, A., Dekoninck, W., Leponce, M., Vanden Spiegel, D. & Semal, P. 2014. Focus stacking: Comparing commercial top-end set-ups with a semi-automatic low budget approach. A possible solution for mass digitization of type specimens. *ZooKeys,* **464**, 1–23. https://doi.org/10.3897/zookeys.464.8615

Bosmans, F., Martin-Eauclaire, M. F. & Tytgat, J. 2006. The scorpion toxin family and its target: An overview. *Toxicon*, **47** (6), 690–699.

Chippaux, J. P. & Goyffon, M. 2008. Epidemiology of scorpionism: A global appraisal. *Acta Tropica*, **107** (2), 71–79.

El-Hennawy, H. K. 1988. Scorpions of Jordan. *Serket*, **1,** 13–20.

El-Hennawy, H. K. 1992. A catalogue of the scorpions described from the Arab countries (1758–1990) (Arachnida: Scorpionida). *Serket*, **2** (4), 95–153.

Fet, V. & Lowe, G. 2000. Family Buthidae C. L. Koch, 1837. *In*: Fet, V., Sissom, W. D., Lowe, G. M. & Braunwalder, E., eds. *Catalog of the Scorpions of the World (1758–1998)*. The New York Entomological Society, New York, NY, 54–286.

Francke, O. F. 1977. Scorpions of the genus *Diplocentrus* from Oaxaca, Mexico (Scorpionida, Diplocentridae). *Journal of Arachnology*, **4,** 145–200.

Hendrixson, B. E. 2006. Buthid scorpions of Saudi Arabia, with notes on other families (Scorpiones: Buthidae, Liochelidae, Scorpionidae). *Fauna of Arabia*, **21,** 33–120.

Hjelle, J. T. 1990. Anatomy and morphology. *In:* Polis, G. A., ed. *Biology of Scorpions.* Stanford University Press, Stanford, CA, 9–63.

Ismail, M. 1995. The treatment of *Androctonus* scorpion envenoming syndrome: New perspectives. *Toxicon*, **33** (7), 825–838.

Kinzelbach, R. 1985. Vorderer Orient. Skorpione (Arachnida: Scorpiones). *Tübingen Atlas der Vorderen Orients (TAVO), Karte A VI 14.2*. Ludwig Reichert Verlag, Wiesbaden.

Levy, G. & Amitai, P. 1980. Scorpiones. *In: Fauna Palaestina, Arachnida I.* Israel Academy of Sciences and Humanities, Jerusalem. 1–130.

Navidpour, S., Kovařík, F., Soleglad, M. E. & Fet, V. 2008. Scorpions of Iran (Arachnida, Scorpiones). Part I. Khoozestan Province. *Euscorpius*, 2008 (**65**), 1–41. https://doi.org/10.18590/euscorpius.2008.vol2008.iss65.1

Rein, J. O. 2025. The Scorpion Files. Trondheim: Norwegian University of Science and Technology. [Accessed 2025 Jan 30]. Available from: https://www.ntnu.no/ub/scorpion-files/.

Seiter, M. & Turiel, C. 2013. First record of *Androctonus australis* (Linnaeus, 1758) from Jordan (Scorpiones: Buthidae). *Revista Ibérica de Aracnología*, **23,** 95–98.

Stahnke, H. L. 1971. Scorpion nomenclature and mensuration. *Entomological News*, **81,** 297–316.

Soleglad, M. E. & Fet, V. 2001. Evolution of Scorpion orthobothriotaxy: A cladistic approach. *Euscorpius*, **1,** 1–38. https://doi.org/10.18590/euscorpius.2001.vol2001.iss1.1

Sousa, P., Arnedo, M. A. & Harris, D. J. 2017. Updated catalogue and taxonomic notes on the Old-World scorpion genus *Buthus* Leach, 1815 (Scorpiones, Buthidae). *ZooKeys*, **686,** 15–84. https://doi.org/10.3897/zookeys.686.12206

Teruel, R. & Kovařík, F. 2014. Redescription of *Androctonus bicolor* Ehrenberg, 1828, and Description of *Androctonus turieli* sp. n. from Tunisia (Scorpiones: Buthidae). *Euscorpius*, **186,** 1–15.

Vachon, M. 1966. Liste des scorpions connus en Égypte, Arabie, Israël, Liban, Syrie, Jordanie, Turquie, Irak, Iran. *Toxicon*, **4** (3), 209–218.

Wahbeh, Y. 1976. A study of Jordanian scorpions. *Jordan Medical Journal*, **11,** 84–92.

Yağmur, E. A. 2021. *Androctonus turkiyensis* sp. n. from the Şanlıurfa Province, Turkey (Scorpiones: Buthidae). *Euscorpius*, **341,** 1–18.

Yağmur, E. A. 2023. *Androctonus kunti* sp. n. from Iğdır Province, Turkey (Scorpiones: Buthidae). *Euscorpius*, **371,** 1–23.

Received 21 March 2025
Accepted 21 October 2025